

Masked Autoencoders are Parameter-Efficient Federated Continual Learners

Yuchen HE*, Xiangfeng WANG†*

*School of Computer Science and Technology, East China Normal University, Shanghai, China 200062

†Shanghai Formal-Tech Information Technology Co., Lt, Shanghai, China 200062

Abstract—Federated learning is a specific distributed learning paradigm in which a central server aggregates updates from multiple clients’ local models, thereby enabling the server to learn without requiring clients to upload their private data, maintaining data privacy. While existing federated learning methods are primarily designed for static data, real-world applications often require clients to learn new categories over time. This challenge necessitates the integration of continual learning techniques, leading to federated continual learning (FCL). To address both catastrophic forgetting and non-IID issues, we propose to use masked autoencoders (MAEs) as parameter-efficient federated continual learners, called pMAE. pMAE learns reconstructive prompt on the client side through image reconstruction using MAE. On the server side, it reconstructs the uploaded restore information to capture the data distribution across previous tasks and different clients, using these reconstructed images to fine-tune discriminative prompt and classifier parameters tailored for classification, thereby alleviating catastrophic forgetting and non-IID issues on a global scale. Experimental results demonstrate that pMAE achieves performance comparable to existing prompt-based methods and can enhance their effectiveness, particularly when using self-supervised pre-trained transformers as the backbone. Code is available at: <https://github.com/ycheoo/pMAE>.

Index Terms—federated continual learning, prompt tuning, self-supervised learning

I. INTRODUCTION

Federated learning [16, 18, 27, 42] is a privacy-preserving decentralized learning paradigm that enables collaborative model training without requiring clients to upload their private data. Traditional federated learning assumes static data, but in real-world scenarios, clients’ data is often dynamic, with old task data being removed and new task data emerging. To address these dynamic scenarios, continual learning [5, 26, 37, 51] techniques need to be integrated into federated learning, a combination known as federated continual learning (FCL) [8, 44], as shown in Figure 1.

In FCL scenarios, new task data is continuously generated on clients, while old task data cannot be fully utilized for model updates. This limitation results in catastrophic forgetting [20, 30], where the model’s performance on previous tasks degrades significantly after training on new tasks. Additionally, due to the non-IID (non-independent and identically distributed) [22, 48] nature of FCL, local data distributions across clients may vary significantly, resulting in a suboptimal global model [22, 46].

This work was supported by the STCSM (22QB1402100) and NSFC (62231019, 12071145). Corresponding author: Xiangfeng Wang.

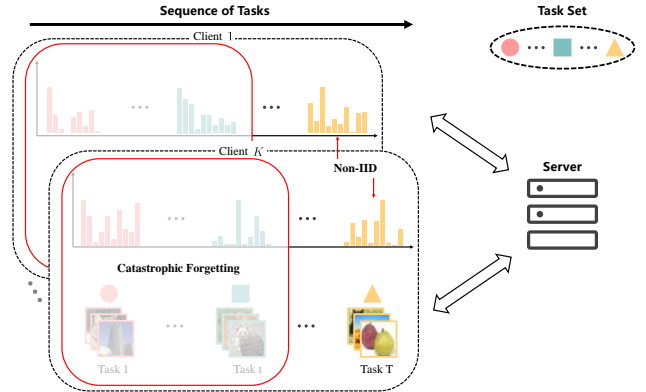


Fig. 1: Illustration of federated continual learning (FCL), wherein clients sequentially learn over T tasks. Each client continuously updates its local model with class-imbalanced private data specific to each task, and further transfers the well-chosen parameters to server for aggregation. The aggregated global model needs to maintain discriminability across all observed classes within the task set.

The performance drop caused by catastrophic forgetting is due to the absence of old task data, which leads the model to overfit the data of current task [20, 30]. Similarly, the performance drop caused by non-IID arises because the local model fits the non-IID data of individual clients, preventing the aggregation of a global model that reflects the overall data distribution [22, 46]. If we could effectively capture the distribution of old task data and account for the differing data distributions across clients, both catastrophic forgetting and the non-IID problem could be significantly alleviated.

Building on the insights from Zhai et al. [45], we propose to use masked autoencoders (MAEs) as parameter-efficient federated continual learners, called pMAE. Originally introduced as scalable vision learners, MAEs [13] leverage self-supervised learning [4, 13, 53] to learn effective visual representations. Instead of focusing solely on representation learning, pMAE emphasizes the ability of MAEs to reconstruct images from restore information. In pMAE, client-side learning not only prioritizes classification as the primary task but also focuses on reconstruction as a secondary task. On the server side, the images reconstructed from uploaded restore information are utilized to fine-tune model parameters tailored for classification. Reconstructed images represent distributions from old tasks and diverse client data, thereby enabling the global mitigation of catastrophic forgetting and non-IID issues.

In FCL, the limitations of client-side computational resources make it burdensome to train a transformer-based model (such as MAEs) [7, 9, 34] from scratch; therefore, we employ pre-trained transformers [12] as the backbone. To further enhance parameter efficiency, we freeze the parameters of the pre-trained transformer and leverage prompt tuning [17, 21]. Specifically, clients utilize discriminative prompt and classifier parameters for classification while employing reconstructive prompt for reconstructing masked images. After completing training, clients randomly extract restore information from a subset of the images and upload them to the server. The server then reconstructs images using reconstructive prompt and restore information, fine-tuning discriminative prompt and classifier parameters in the process, which mitigates performance degradation from catastrophic forgetting and non-IID issues on a global scale. Given the generality of our approach, it can be directly integrated with existing prompt-based methods [31, 38, 39] to enhance their performance.

Our contributions can be summarized as follows:

- We propose to use masked autoencoders (MAEs) for FCL tasks, mitigating catastrophic forgetting and non-IID issues globally by reconstructing images on the server.
- We introduce prompt tuning as a parameter-efficient method for fine-tuning pre-trained transformers, employing discriminative prompt for the classification task and reconstructive prompt for the reconstruction task.
- Experimental results indicate that pMAE achieves performance comparable to existing prompt-based methods and can be directly integrated to enhance their effectiveness, particularly when utilizing self-supervised pre-trained transformers as the backbone.

II. RELATED WORK

A. Continual Learning

Continual learning, also known as incremental learning or lifelong learning [5, 26, 37, 51], is a learning paradigm in which models acquire knowledge from a series of sequential tasks. This approach is typically categorized into three main types: Regularization-based methods [20, 24, 32], which limit changes to model parameters during the learning of new tasks; Rehearsal-based methods [30, 40, 45], which involve revisiting historical data from previous tasks while learning new ones; Model expansion-based methods [41, 43, 49], which incorporate additional network structures when acquiring new tasks.

Recent advances in continual learning have introduced approaches that leverage knowledge from pre-trained transformers [7, 9, 34] through parameter-efficient tuning [3, 15, 17, 21, 23]. In particular, prompt-based methods [25, 31, 36, 38, 39] instruct pre-trained transformers using lightweight prompts [17, 21, 23]. EASE [52] trains a unique adapter module [3] for each task, aiming to develop task-specific subspaces. ADAM [50] and LAE [10] propose general continual learning frameworks, which can be smoothly integrated with other parameter-efficient tuning methods.

B. Federated Continual Learning

Federated learning is a decentralized learning paradigm where multiple clients jointly build a global model without exchanging their personal data [16, 18, 27, 42]. Nevertheless, this learning paradigm typically presupposes that clients' data does not change, overlooking the reality that data tends to evolve and grow over time.

Federated continual learning (FCL) [8, 44] seeks to tackle the challenge of enabling clients to learn progressively across multiple tasks by integrating continual learning techniques into the federated learning framework. FCL faces obstacles such as catastrophic forgetting [20, 30], a known issue in continual learning, and the non-IID issue [22, 48] common in federated learning.

In recent years, the field of FCL has experienced significant growth [8, 29, 44, 47]. With the rise of pre-trained models [12], FCL approaches leveraging parameter-efficient tuning [3, 15, 17, 21, 23] on pre-trained transformers [7, 9, 34] have demonstrated impressive performance while reducing communication overhead. Fed-CPrompt [1], employing prompting techniques [17, 21, 23], enables communication-efficient FCL without the need for data rehearsal. Powder [28] is designed to promote effective knowledge transfer encapsulated in prompts across sequentially learned tasks and different clients. PILoRA [11], which incorporates LoRA [15] and prototype [33], enhances representation learning and utilizes heuristic information between prototypes and class features.

III. PRELIMINARIES

A. Problem Definition

In FCL [8, 44], a server oversees a group of K clients that sequentially learn across T tasks. Training data is randomly assigned to clients and cannot be shared or uploaded. This work primarily focuses on addressing the challenges of class-incremental learning [30] within the context of continual learning. Class-incremental learning involves handling T sets of non-overlapping, class-labeled datasets, denoted as $\{\mathcal{D}^1, \dots, \mathcal{D}^T : \mathcal{D}^t = (x_i^t, y_i^t)_{i=1}^{n^t}\}$, where \mathcal{D}^t is the training dataset for the t -th task, and $y_i^t \in \mathcal{Y}^t$ refers to the class label corresponding to x_i^t . For any two distinct tasks, the class sets are mutually exclusive, represented as $\mathcal{Y}^t \cap \mathcal{Y}^{t'} = \emptyset$ for $t \neq t'$. During the training of task t , updates can only be made using \mathcal{D}^t or a limited amount of rehearsal data [30]. The updated model must classify all classes encountered across the first t tasks, i.e., $\cup_{i=1}^t \mathcal{Y}^i$.

When extending class-incremental learning to a federated learning setting, the training data for the t -th task is distributed randomly across K clients, represented as $\mathcal{D}^t = \{\mathcal{D}_k^t\}_{k=1}^K$. For any two clients $k \neq k'$, their datasets are disjoint, meaning $\mathcal{D}_k^t \cap \mathcal{D}_{k'}^t = \emptyset$.

B. Masked Autoencoders

Masked Autoencoders (MAEs) were originally introduced as scalable vision learners in a self-supervised paradigm by reconstructing images from masked inputs [13].

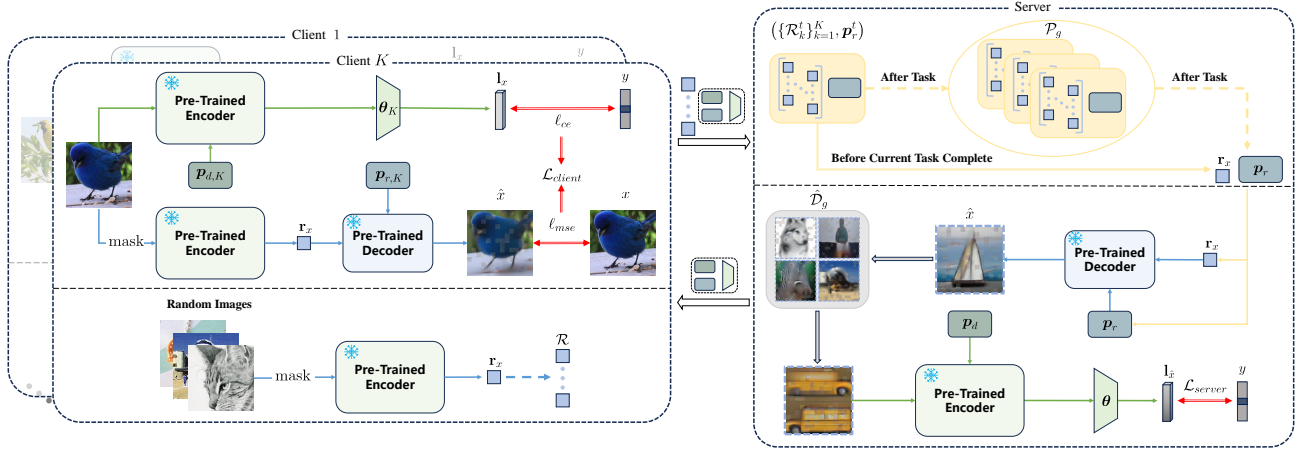


Fig. 2: The overview of proposed pMAE framework. 1) Client: Extract labeled restore information using Eq. (3) and optimize prompts and classifier parameters of the local model by \mathcal{L}_{client} . 2) Server: Generate reconstructed images using Eq. (4) and fine-tune discriminative prompt and classifier parameters of the aggregated global model by \mathcal{L}_{server} . 3) Lightweight prompts, classifier parameters and labeled restore information are transmitted between clients and the server, while no additional data is stored on each client. 4) Images are reconstructed into tensors and subsequently used for fine-tuning, ensuring that **no real images are stored on the server**.

The MAE encoder is a Vision Transformer (ViT) model [9], where input images are divided into non-overlapping patches, and a significant portion (e.g., 75 %) of these patches are randomly masked. The remaining unmasked patches are encoded into visible tokens and passed to the decoder along with restore ids, which indicate the positions of masked tokens.

The MAE decoder, which is used only for reconstruction task during the pre-training stage, is designed much narrower and shallower than the encoder. The visible tokens from the encoder are combined with learnable mask tokens that replace the masked patches based on restore ids. The decoder then processes the combination of visible tokens and mask tokens to reconstruct the original input images in the pixel space.

C. Prompt Tuning

Prompt tuning [17, 21] is a parameter-efficient method for tuning pre-trained transformers [7, 9, 34], where a prompt parameter $\mathbf{p} \in \mathbb{R}^{L_p \times D}$, with L_p representing the sequence length and D denoting the embedding dimension, is prepended to the encoded feature \mathbf{h} of input x . Specifically, an identical \mathbf{p} is prepended to the query, key, and value of encoded feature \mathbf{h} , denoted as \mathbf{h}_Q , \mathbf{h}_K , and \mathbf{h}_V , respectively. This prepending occurs within the multi-head self-attention (MSA) layers and is expressed as:

$$\text{MSA}([\mathbf{p}; \mathbf{h}_Q], [\mathbf{p}; \mathbf{h}_K], [\mathbf{p}; \mathbf{h}_V]) \quad (1)$$

where $[\cdot; \cdot]$ denotes the concatenation operation along the sequence length.

In pMAE, we introduce a discriminative prompt for classification and a reconstructive prompt for image reconstruction. Following prior works [31, 38, 39], the discriminative prompt length is set to $L_p = 20$ and is inserted into the first five transformer blocks with individual parameters. The reconstructive prompt is set with $L_p = 5$ and is only inserted into the first layer, which we designed specifically.

IV. METHODOLOGY OF THE pMAE

In FCL, the performance is influenced by two key issues: catastrophic forgetting and non-IID, which are caused by the absence of old task data and varying local data distributions. To tackle catastrophic forgetting and non-IID issues in a parameter-efficient manner, pMAE utilizes the reconstruction ability of MAEs and the instruction ability of prompt tuning.

On the client side, pre-trained transformers learn from prompt tuning, where discriminative prompt enhance the classification performance of the encoder, and reconstructive prompt improve the reconstruction performance of the decoder. Restore information, along with tuned model parameters, are then extracted and uploaded to the server.

On the server side, the received restore information and reconstructive prompt are used to reconstruct images, which are subsequently used to fine-tune the discriminative prompt and classifier parameters, mitigating catastrophic forgetting and non-IID issues from a global perspective.

A. Client Side: Learning from Prompting

The backbone of the local model consists of a pre-trained transformer encoder F_Φ and a pre-trained transformer decoder G_ψ , with the model parameters Φ and ψ remaining frozen. To instruct pre-trained transformers and obtain output logits for classification, tunable prompts and classifier are introduced.

Specifically, for the classification task, there are a discriminative prompt \mathbf{p}_d and a classifier H_θ parameterized by θ . As described in Sec III-C, prompt \mathbf{p} is prepended to the encoded feature \mathbf{h} of input x . For convenience, we use $[\cdot, \cdot]$ to denote such combination. The output logits can then be denoted as:

$$\mathbf{l}_x = H_\theta(F_\Phi([\mathbf{p}_d, x])), \quad (2)$$

and the classification loss is computed using the cross-entropy (CE) between the ground truth y and the output logits \mathbf{l}_x , denoted as $\ell_{ce}(\mathbf{l}_x, y)$.

Similarly, for the reconstruction task, we have a reconstructive prompt \mathbf{p}_r , which is utilized to enhance the decoder’s reconstruction performance. During the learning process, input images x are masked with a portion of 75 % and encoded by the pure encoder F_Φ without discriminative prompt \mathbf{p}_d as:

$$\mathbf{r}_x = F_\Phi(\text{mask}(x)), \quad (3)$$

where \mathbf{r}_x represents the restore information, which includes the encoded visible tokens and the restore ids of the masked input images $\text{mask}(x)$.

The decoder, G_ψ , subsequently outputs the reconstructed images with the reconstructive prompt \mathbf{p}_r as:

$$\hat{x} = G_\psi([\mathbf{r}_x, \mathbf{p}_r]), \quad (4)$$

where \hat{x} represents the reconstructed version of the original images x , and the loss of reconstruction is computed as the mean squared error (MSE) between the reconstructed and original images in pixel space, denoted by $\ell_{mse}(\hat{x}, x)$.

To summarize the modeling process above, the overall loss function for each client is:

$$\mathcal{L}_{client}(\mathbf{p}_d, \boldsymbol{\theta}, \mathbf{p}_r) = \sum_{(x,y) \in \mathcal{D}_k^t} (\ell_{ce}(\mathbf{l}_x, y) + \ell_{mse}(\hat{x}, x)). \quad (5)$$

where \mathcal{D}_k^t represents the private dataset of client k at task t .

Once the training process is complete, clients will randomly selects a number of u images and extracts their labeled restore information, represented as $\mathcal{R} = \{(\mathbf{r}_{x_i}, y_i)\}_{i=1}^u$, which will be uploaded to the server for global image reconstruction. Ultimately, clients uploads only the prompts \mathbf{p}_d and \mathbf{p}_r , the classifier parameters $\boldsymbol{\theta}$, and the labeled restore information \mathcal{R} to the server, which are significantly more lightweight than the model parameters of encoder and decoder. For clarity of notation, transmitted model parameters are collectively expressed as $\mathbf{w} = \{\mathbf{p}_d, \boldsymbol{\theta}, \mathbf{p}_r\}$.

B. Server Side: Fine-tuning from Reconstructing

The discriminative prompt \mathbf{p}_d and classifier parameters $\boldsymbol{\theta}$ uploaded by the client can be aggregated by FedAvg [27] to form a global model for classification. However, the performance of the global model may be compromised due to catastrophic forgetting caused by the absence of old task data, as well as non-IID issue arising from varying local distributions. Therefore, it is essential to utilize the reconstructive prompt \mathbf{p}_r and the labeled restore information \mathcal{R} to capture distributions from old tasks and diverse clients.

For the labeled restore information uploaded by clients, the server will aggregates it into $\{\mathcal{R}_k\}_{k=1}^K$, which, along with the FedAvg-aggregated reconstructive prompt \mathbf{p}_r , is denoted as $(\{\mathcal{R}_k\}_{k=1}^K, \mathbf{p}_r)$ for image reconstruction. Since $\{\mathcal{R}_k\}_{k=1}^K$ contains distribution information from different clients, it can effectively mitigate the non-IID issue. Specifically, based on Eq. (4), the reconstructive prompt \mathbf{p}_r is used to reconstruct the labeled image (\hat{x}, y) with labeled restore information (\mathbf{r}_x, y) from $\{\mathcal{R}_k\}_{k=1}^K$, creating a reconstructed global dataset $\hat{\mathcal{D}}_g$.

Algorithm 1 The pMAE Framework

Input: communication rounds per task R , local epochs E , number of clients K , private datasets $\{\mathcal{D}_k^t\}_{k=1}^K$.

```

1: procedure pMAE
2:   Initialize  $\mathbf{w} = \{\mathbf{p}_d, \boldsymbol{\theta}, \mathbf{p}_r\}$ , restore pool  $\mathcal{P}_g = \{\}$ ;
3:   for each task  $t = 1, 2, \dots, R$  do
4:     for  $\tau = 1, 2, \dots, R$  do
5:       for  $k = 1, 2, \dots, K$  in parallel do
6:          $\mathbf{w}_k^{\tau+1}, \mathcal{R}_k^t \leftarrow \text{LOCALUPDATE}(t, k, \mathbf{w}^\tau)$ ;
7:       end for
8:        $\mathbf{w}^{\tau+1} \leftarrow \sum_{k=1}^K \frac{|\mathcal{D}_k^t|}{|\mathcal{D}^t|} \mathbf{w}_k^{\tau+1}$ ;
9:       if  $\tau \neq R$  then
10:        Generate  $\hat{\mathcal{D}}_g$  with  $(\{\mathcal{R}_k^t\}_{k=1}^K, \mathbf{p}_r^{\tau+1})$ ;
11:        Optimize  $\mathbf{p}_d^{\tau+1}, \boldsymbol{\theta}^{\tau+1}$  by Eq. (6);
12:       end if
13:     end for
14:      $\mathcal{P}_g \leftarrow \mathcal{P}_g \cup (\{\mathcal{R}_k^t\}_{k=1}^K, \mathbf{p}_r^t)$ ;
15:     Generate  $\hat{\mathcal{D}}_g$  with  $\mathcal{P}_g = \{(\{\mathcal{R}_k^i\}_{k=1}^K, \mathbf{p}_r^i)\}_{i=1}^t$ ;
16:     Optimize  $\mathbf{p}_d^t, \boldsymbol{\theta}^t$  by Eq. (6);
17:   end for
18: end procedure

19: function LOCALUPDATE( $t, k, \mathbf{w}$ )
20:    $\mathbf{w}_k = \{\mathbf{p}_{d,k}, \boldsymbol{\theta}_k, \mathbf{p}_{r,k}\} \leftarrow \mathbf{w}$ ;
21:   for  $e = 1, 2, \dots, E$  do
22:     for  $(x, y)$  in  $\mathcal{D}_k^t$  do
23:       Optimize  $\mathbf{w}_k$  by Eq. (5);
24:     end for
25:   end for
26:   Extract labeled restore information  $\mathcal{R}_k^t$  by Eq. (3);
27:   return  $\mathbf{w}_k, \mathcal{R}_k^t$ .
28: end function

```

This reconstructed global dataset is then used to fine-tune the discriminative prompt and classifier parameters as:

$$\mathcal{L}_{server}(\mathbf{p}_d, \boldsymbol{\theta}) = \sum_{(\hat{x}, y) \in \hat{\mathcal{D}}_g} \ell_{ce}(\mathbf{l}_{\hat{x}}, y). \quad (6)$$

However, due to the absence of old task data, the issue of catastrophic forgetting remains unresolved. Therefore, we propose using a restore pool \mathcal{P}_g to save past data distributions. Specifically, after task t is completed, the aggregated labeled restore information and reconstructive prompt are merged into the restore pool as: $\mathcal{P}_g \leftarrow \mathcal{P}_g \cup (\{\mathcal{R}_k^t\}_{k=1}^K, \mathbf{p}_r^t)$. Here, $\{\mathcal{R}_k^t\}_{k=1}^K$ and \mathbf{p}_r^t are the aggregated labeled restore information and reconstructive prompt after the completion of task t , which encompass the data distribution of task t .

During the subsequent server fine-tuning, if the current task is still ongoing, $(\{\mathcal{R}_k\}_{k=1}^K, \mathbf{p}_r)$ is utilized for image reconstruction. If the current task has ended, the aggregated labeled restore information and reconstructive prompt are merged into the restore pool \mathcal{P}_g . We then use $\mathcal{P}_g = \{(\{\mathcal{R}_k^i\}_{k=1}^K, \mathbf{p}_r^i)\}_{i=1}^t$, which contains both old task data and current task data, to generate a reconstructed global dataset $\hat{\mathcal{D}}_g$ and use Eq. (6) to fine-tune the discriminative prompt and classifier parameters.

V. EXPERIMENTS

A. Experimental Setup

Datasets and Non-IID Setting. To evaluate the performance of pMAE in FCL scenarios, two representative benchmark datasets are utilized: CUB-200 [35] and ImageNet-R [14]. These datasets are randomly divided into 20 tasks ($T = 20$), with each task containing an equal number of distinct classes. The CUB-200 dataset comprises approximately 12,000 images spanning 200 fine-grained bird categories. The ImageNet-R dataset includes 200 classes with 24,000 training images and 6,000 testing images, with all considered out-of-distribution data, despite sharing some classes with ImageNet [6], the dataset used for pre-training. Consequently, ImageNet-R is widely used in recent continual learning research based on pre-trained models [31, 38].

To simulate a non-IID environment, the Dirichlet distribution is applied, a standard approach in federated learning [22, 46]. The degree of non-IIDness is controlled by the parameter β , with lower values indicating a greater degree of non-IID distribution. Notably, by employing this partitioning strategy, the private data for each client may include majority, minority, or missing classes, which could reflect real-world complexities.

Evaluation Metric. In evaluating method performance, the metrics of accuracy A_t and average accuracy \bar{A} are employed, as established in [2] and widely adopted in continual learning [31, 38, 39]. The accuracy on task i after learning task t is denoted as $a_{i,t}$, and $A_t = \frac{1}{t} \sum_{i=1}^t a_{i,t}$ represents the accuracy of all tasks after learning task t . The overall performance after task T is quantified through the calculation of average accuracy $\bar{A} = \frac{1}{T} \sum_{t=1}^T A_t$, where T signifies the total number of tasks, thus providing a comprehensive measure across the entire learning progression.

Baselines. Our pMAE is compared with three continual learning methods that utilize prompts: L2P [39], DualPrompt [38], and CODA-Prompt [31]. Notably, these continual learning techniques will be adapted to the FCL setting, referred to as FedL2P, FedDualP, and FedCODA-P, respectively.

Implementation Details. The Adam optimizer [19] is applied across all methods, utilizing a consistent batch size of 128 and a learning rate of $lr = 1e^{-3}$. The number of clients is set to $K = 10$, with a total of $R_{all} = 200$ communication rounds and local update epochs $E = 5$. For each task, communication rounds are determined as $R = \frac{R_{all}}{T}$. For pMAE, the uploaded number of restore information is set to $u = 4$, and fine-tuning on the server is performed over $E_{server} = 5$ epochs.

All experiments are conducted across three random seeds 2023, 2024, and 2025, with the final results derived from them.

Pre-training of Decoder. Previous works [31, 38, 39] all use a ViT-B/16 model pre-trained on ImageNet [6] as a supervised learning (Sup) backbone. We also consider iBOT [53], which employs a self-supervised learning paradigm [4, 13, 53]. Since our pMAE requires both an encoder for representation and a decoder for reconstruction, it necessitates pre-training a suitable decoder on both Sup and iBOT pre-trained encoders.

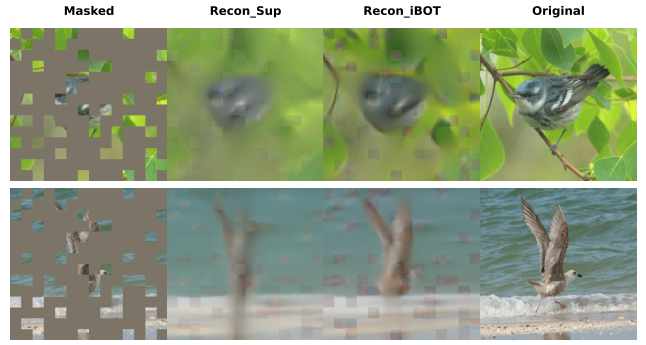


Fig. 3: **Uncurated random samples** of CUB-200 images, using an MAE trained on ImageNet-100 with frozen pre-trained encoder. For each quadruplet, we show the masked image, Sup-based MAE reconstruction, iBOT-based MAE reconstruction, and the ground-truth. The masking ratio is 75%.

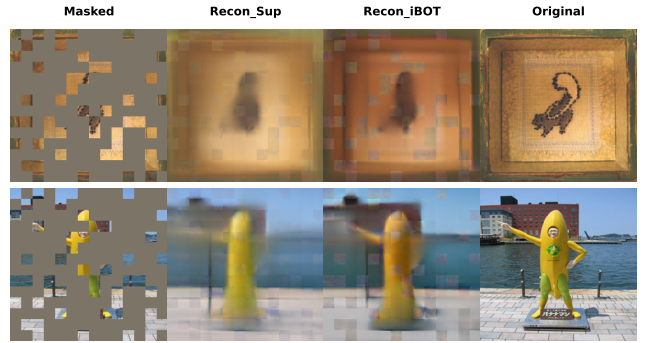


Fig. 4: **Uncurated random samples** of ImageNet-R images, using an MAE trained on ImageNet-100 with frozen pre-trained encoder. For each quadruplet, we show the masked image, Sup-based MAE reconstruction, iBOT-based MAE reconstruction, and the ground-truth. The masking ratio is 75%.

Specifically, the ImageNet-100 dataset [40], a subset of 100 classes from ImageNet [6], is utilized for pre-training. We adopt the original MAE pre-training paradigm, which inputs images with 75% masking into the encoder and performs reconstruction with the decoder. Our aim is to develop a decoder capable of reconstruction while maintaining the encoder’s performance, ensuring fairness in comparisons with other methods. Therefore, we freeze the encoder during pre-training and optimize only the decoder. In the original MAE pre-training, the primary objective is to obtain an encoder that produces representations for recognition. However, since a pre-trained encoder is already employed, 200 epochs of iterations have already achieved convergence in our experiments.

Notably, in the original paper [13], the reconstruction target is the normalized pixels of each masked patch, which improves representation but reduces reconstruction quality. To focus on reconstruction, we use unnormalized pixels as the target.

Figure 3 and Figure 4 show the reconstruction results of the Sup-based MAE and the iBOT-based MAE on CUB-200 and ImageNet-R datasets. From the reconstruction perspective, the iBOT-based MAE, which uses a self-supervised pre-trained encoder, outperforms the Sup-based MAE.

TABLE I: **Results on 20-task CUB-200.** \bar{A} gives the accuracy averaged over tasks, A_T gives the final accuracy of all tasks. We report results over 3 trials.

PTM	Method	$\beta = 0.5$		$\beta = 0.1$		$\beta = 0.05$	
		\bar{A} (\uparrow)	A_T (\uparrow)	\bar{A} (\uparrow)	A_T (\uparrow)	\bar{A} (\uparrow)	A_T (\uparrow)
Sup	FedL2P	58.14 \pm 5.19	41.55 \pm 1.07	40.20 \pm 3.09	25.31 \pm 0.83	33.38 \pm 1.14	22.89 \pm 1.76
	FedDualP	66.16 \pm 2.22	49.63 \pm 0.65	46.24 \pm 1.36	30.36 \pm 2.35	41.03 \pm 2.65	26.22 \pm 0.83
	FedCODA-P	65.58 \pm 1.93	47.86 \pm 1.26	47.97 \pm 2.06	32.08 \pm 1.84	43.98 \pm 2.89	27.04 \pm 2.20
	pMAE	77.18\pm1.22	63.80\pm0.07	68.93\pm1.77	55.84\pm0.84	66.12\pm0.75	51.85\pm1.59
iBOT	FedL2P	14.08 \pm 1.83	6.34 \pm 0.75	6.89 \pm 0.47	2.46 \pm 0.7	5.53 \pm 0.14	2.5 \pm 0.52
	FedDualP	31.57 \pm 3.83	16.76 \pm 0.95	18.06 \pm 1.05	8.46 \pm 1.47	15.13 \pm 1.32	7.83 \pm 2.17
	FedCODA-P	38.88 \pm 3.43	23.00 \pm 1.02	21.7 \pm 1.12	10.32 \pm 1.83	18.7 \pm 1.02	9.86 \pm 1.16
	pMAE	53.19\pm1.21	39.35\pm0.78	43.32\pm1.93	32.55\pm1.02	40.69\pm1.45	30.15\pm0.87

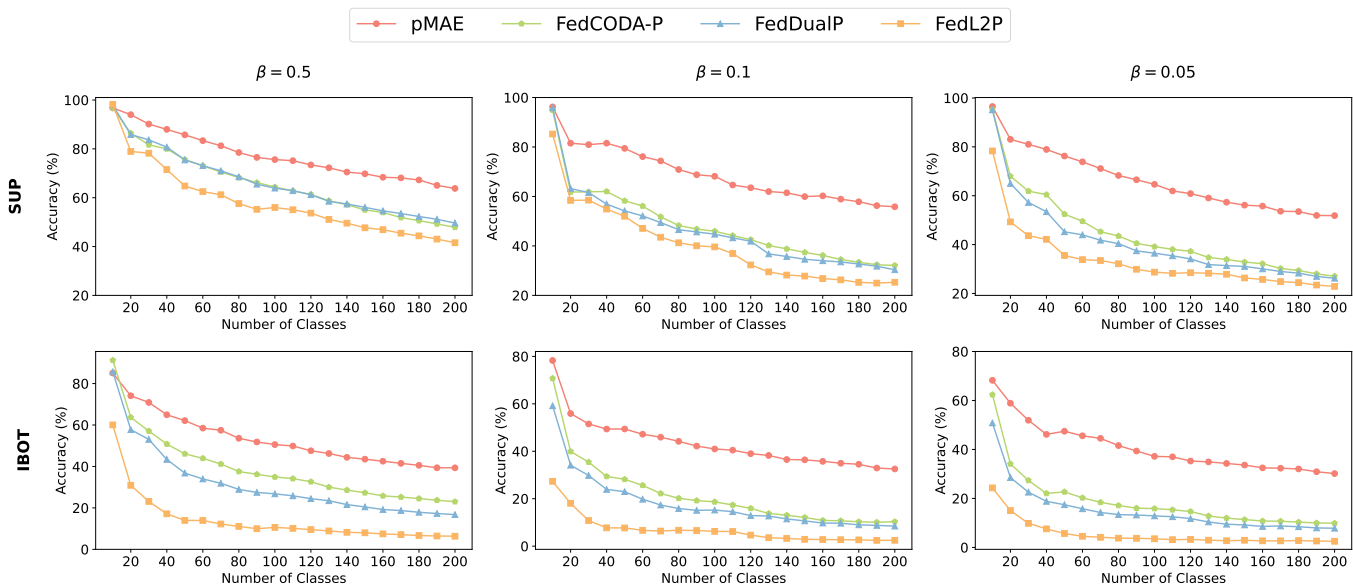


Fig. 5: Accuracy curves on 20-task CUB-200.

B. Performance Comparison

Experiments were conducted on CUB-200 and ImageNet-R datasets with a fixed number of tasks $T = 20$, where each task comprises 10 classes. With a number of clients $K = 10$, we varied non-IID degrees $\beta \in \{0.5, 0.1, 0.05\}$ to examine the impact on performance and the non-IID robustness of all methods. Table I and Table II respectively present the results for CUB-200 and ImageNet-R across the average accuracy \bar{A} and last stage accuracy A_T metrics. Figure 5 and Figure 4 display the accuracy A_t at each task stage t under different pre-trained models (PTMs) and varying non-IID degrees.

In Table I, our pMAE approach achieves optimal performance levels on the CUB-200 dataset across different non-IID degrees and pre-trained models. Furthermore, Figure 5 illustrates more intuitively that as the degree of non-IID increases, the performance disparity between pMAE and the other methods becomes even more pronounced.

It is noteworthy that when the pre-trained model is based on iBOT, the performance gap between pMAE and the other methods becomes larger compared to the Sup-based model. This may be attributed to their key-query matching mechanism, which limits performance when using a self-supervised pre-trained model as the backbone.

L2P [39] introduced a key-query matching mechanism for selecting prompts from a prompt pool to instruct pre-trained transformers. Building on L2P, DualPrompt [38] enhanced performance by incorporating both general prompts and expert prompts. CODA-Prompt [31] utilizes an attention mechanism to construct input-conditioned prompts.

Their commonality lies in relying on a pre-trained encoder to calculate query and construct prompts for classification based on the calculated query, with the constructed prompts serving a role similar to the discriminative prompt proposed in our pMAE. Since the construction of prompts is based on calculated query, these methods heavily depend on the discriminative performance of the pre-trained encoder, which serves as a frozen feature extractor.

In our experiments, the Sup-based model aligns with the backbone used in [31, 38, 39], which exhibits strong discriminative performance. In contrast, the iBOT-based model, which employs a self-supervised pre-training paradigm, has weaker discriminative ability, resulting in performance degradation. However, our pMAE directly defines the discriminative prompt without construction, leading to only minimal performance degradation when using the self-supervised pre-trained iBOT-based model.

TABLE II: **Results on 20-task ImageNet-R.** \bar{A} gives the accuracy averaged over tasks, A_T gives the final accuracy of all tasks. We report results over 3 trials.

PTM	Method	$\beta = 0.5$		$\beta = 0.1$		$\beta = 0.05$	
		\bar{A} (\uparrow)	A_T (\uparrow)	\bar{A} (\uparrow)	A_T (\uparrow)	\bar{A} (\uparrow)	A_T (\uparrow)
Sup	FedL2P	48.83 \pm 4.77	41.37 \pm 1.07	28.47 \pm 3.53	18.39 \pm 3.64	24.99 \pm 2.56	16.01 \pm 3.31
	FedDualP	56.17 \pm 1.84	48.58 \pm 0.65	37.25 \pm 0.65	28.61 \pm 2.84	31.71 \pm 5.31	21.80 \pm 3.13
	FedCODA-P	59.56 \pm 2.76	52.40\pm1.61	39.27 \pm 1.55	30.01 \pm 3.37	33.86 \pm 4.63	23.61 \pm 2.13
	pMAE	60.04\pm0.17	50.89 \pm 1.36	53.55\pm2.10	46.31\pm2.26	46.72\pm3.45	39.98\pm1.75
iBOT	FedL2P	21.18 \pm 2.06	22.14 \pm 0.53	10.45 \pm 0.83	8.25 \pm 1.01	9.92 \pm 1.08	6.86 \pm 0.11
	FedDualP	41.90 \pm 1.94	35.26 \pm 1.55	24.71 \pm 0.51	18.12 \pm 2.30	21.90 \pm 2.06	14.66 \pm 1.47
	FedCODA-P	50.28 \pm 2.46	43.08 \pm 0.77	30.34 \pm 1.00	22.44 \pm 2.41	26.53 \pm 2.81	17.53 \pm 2.16
	pMAE	53.47\pm0.79	46.90\pm0.51	47.78\pm0.72	43.13\pm0.52	42.65\pm3.44	38.86\pm0.59

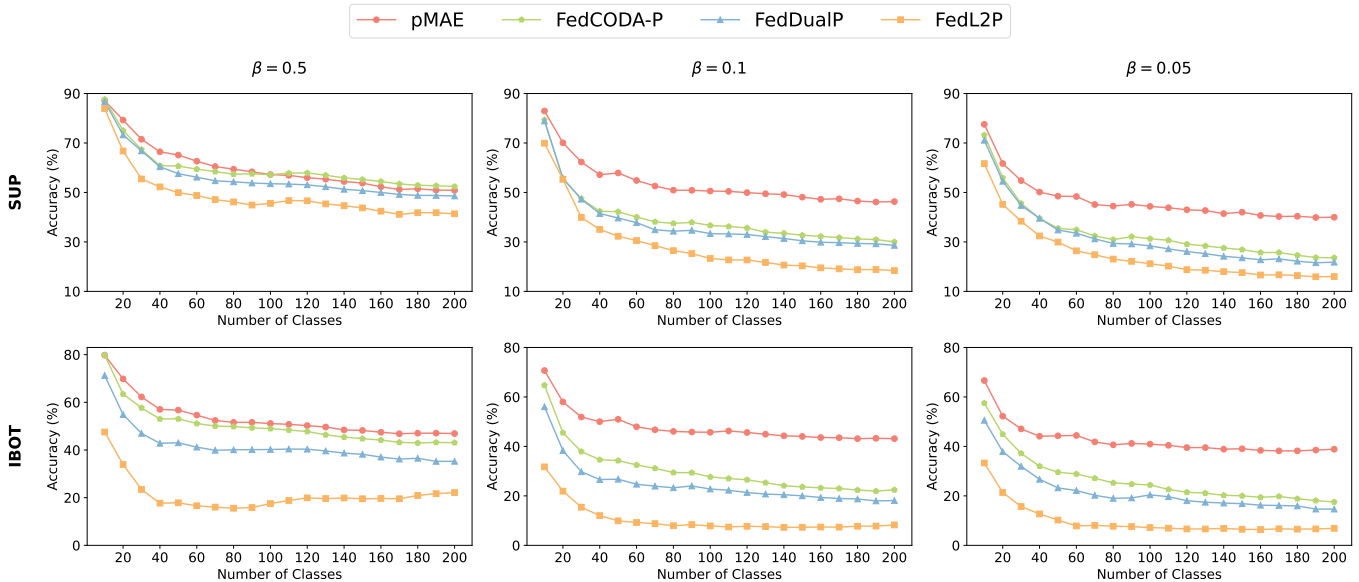


Fig. 6: Accuracy curves on 20-task ImageNet-R.

For ImageNet-R dataset, as shown in Table II and Figure 6, when using the Sup-based model with $\beta = 0.5$ (indicating a relatively low non-IID degree), pMAE achieves an average accuracy \bar{A} comparable to FedCODA-P and FedDualP, while FedCODA-P achieves a higher final accuracy A_t . This may be attributed to the out-of-distribution characteristic of ImageNet-R dataset. FedCODA-P and FedDualP utilize specific prompts to retain knowledge acquired from each task. Consequently, they are better suited to handle the out-of-distribution data in ImageNet-R, allowing for both the learning and preserving of each task’s distinct distribution. In contrast, pMAE employs a single discriminative prompt, which may limit its capability to handle the out-of-distribution data in ImageNet-R.

Although the out-of-distribution data in ImageNet-R limits the effectiveness of the discriminative prompt, the mechanism of using restore information for reconstruction on the server to fine-tune the discriminative prompt and classifier parameters enables pMAE to effectively mitigate performance degradation caused by catastrophic forgetting and non-IID issues, allowing it to achieve optimal performance in other settings. Furthermore, as the non-IID degree increases, the performance gap between pMAE and other methods becomes more significant, consistent with the observations from CUB-200.

C. Enhancing Other Methods with pMAE

The generality of pMAE enables seamless integration with existing prompt-based methods [31, 38, 39] to enhance performance. Since these methods already utilize an encoder for feature extraction, integrating pMAE simply requires adding a decoder to establish a complete MAE. During client training, the reconstructive prompt is optimized with MSE loss (as outlined in Section IV). Restore information is then extracted on the client, uploaded to the server, and used with the reconstructive prompt for reconstruction. These reconstructed images are subsequently used for fine-tuning parameters tailored for classification, without any further modifications.

The experimental results, presented in Figure 7 and Figure 8, show that FedCODA-P, FedDualP, and FedL2P achieve substantial performance improvements across different pre-trained models and non-IID degrees, especially when using an iBOT-based model. It is noteworthy that the y-axis starting points in Figure 7 and Figure 8 differ. Despite the bars appear lower in Figure 7, the Sup-based model actually performs better than the iBOT-based model.

Additionally, as indicated by the slope, integrating pMAE reduces the rate of performance decline as non-IID degree increases, underscoring pMAE’s contribution to robustness.

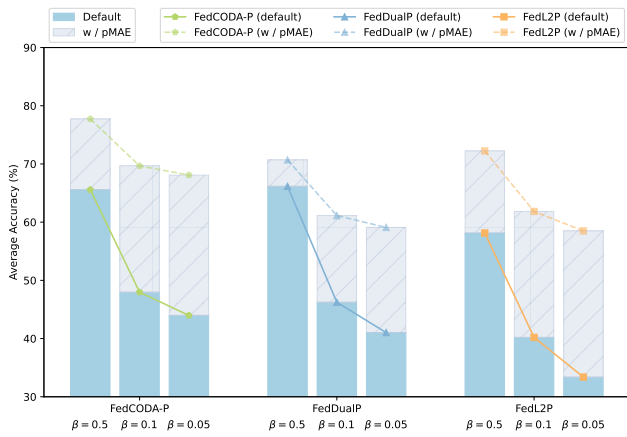


Fig. 7: **Sup-based** improvement of other methods with pMAE for average accuracy \bar{A} on 20-task CUB-200.

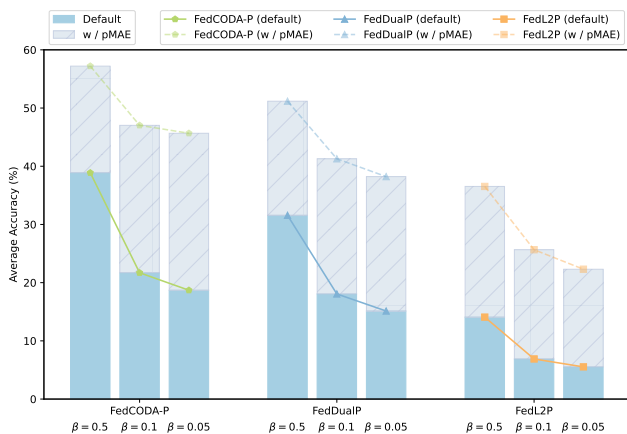


Fig. 8: **iBOT-based** improvement of other methods with pMAE for average accuracy \bar{A} on 20-task CUB-200.

D. Ablation Study

To better understand the effects of individual components of pMAE, we perform an ablation study on CUB-200 dataset. Table III and Table IV offer insights into the impact of ablating reconstructive prompt, reducing restoration information, and removing restoration pool.

Specifically, the ablation of reconstructive prompt results in a decline in the quality of image reconstructed on the server side. As shown in Figures 9 and 10, image reconstructed with reconstructive prompt exhibit superior quality, which is crucial for the fine-tuning process on the server side. The reconstructive prompt offers a more significant quality improvement for the Sup-based model compared to the iBOT-based model, which can also be confirmed by the performance degradation resulting from ablating reconstructive prompt in Tables III and IV.

The default number of uploaded restore information is set to $u = 4$, we reduce it to $u = 1$ to assess its impact on the performance of pMAE. It is observed that reducing restore information resulted in a more pronounced drop in average accuracy compared to ablating reconstructive prompt.



Fig. 9: **Sup-based** reconstruction of an example from CUB-200 images. For each quadruplet, we show the masked image, unprompted reconstruction, prompted reconstruction, and the ground-truth. The masking ratio is 75%.



Fig. 10: **iBOT-based** reconstruction of an example from CUB-200 images. For each quadruplet, we show the masked image, unprompted reconstruction, prompted reconstruction, and the ground-truth. The masking ratio is 75%.

TABLE III: **Sup-based** ablation results for average accuracy \bar{A} on 20-task CUB-200.

Method	$\beta = 0.5$	$\beta = 0.1$	$\beta = 0.05$
pMAE	77.18\pm1.22	68.93\pm1.77	66.12\pm0.75
Ablate Reconstructive Prompt	74.19 \pm 2.49	65.27 \pm 2.28	62.21 \pm 4.00
Reduce Restore Information	68.74 \pm 2.66	57.16 \pm 4.15	55.00 \pm 2.70
Remove Restore Pool	65.36 \pm 2.36	54.45 \pm 3.91	51.20 \pm 4.86

TABLE IV: **iBOT-based** ablation results for average accuracy \bar{A} on 20-task CUB-200.

Method	$\beta = 0.5$	$\beta = 0.1$	$\beta = 0.05$
pMAE	53.19\pm1.21	43.32\pm1.93	40.69\pm1.45
Ablate Reconstructive Prompt	52.92 \pm 1.42	43.15 \pm 2.09	40.39 \pm 1.14
Reduce Restore Information	47.25 \pm 2.30	35.51 \pm 1.92	31.74 \pm 1.05
Remove Restore Pool	39.06 \pm 3.90	27.44 \pm 1.05	27.77 \pm 2.51

Remarkably, the removal of restore pool incurs a significant decline in average accuracy, emphasizing its pivotal role in retaining distributions from old task data, which is a major factor leading to catastrophic forgetting in FCL.

VI. CONCLUSION

In this work, we propose to use masked autoencoders (MAEs) as parameter-efficient federated continual learners, called **pMAE**. Our pMAE effectively addresses the challenges of catastrophic forgetting and non-IID issues by employing the image reconstruction ability of MAEs. Specifically, on the client side, pMAE learns a reconstructive prompt through reconstruction. On the server side, it aggregates uploaded restore information and reconstructs images with the reconstructive prompt to capture data distributions across tasks and clients. Experiments conducted on benchmark datasets demonstrate the effectiveness of pMAE, showing competitive performance compared to existing prompt-based methods and highlighting its ability to enhance their capabilities, particularly when using self-supervised pre-trained transformers.

REFERENCES

- [1] Gaurav Bagwe, Xiaoyong Yuan, Miao Pan, and Lan Zhang. Fed-CPrompt: Contrastive prompt for rehearsal-free federated continual learning. In *Federated Learning and Analytics in Practice: Algorithms, Systems, Applications, and Opportunities*, 2023.
- [2] Arslan Chaudhry, Puneet K Dokania, Thalaiyasingam Ajanthan, and Philip HS Torr. Riemannian walk for incremental learning: Understanding forgetting and intransigence. In *ECCV*, 2018.
- [3] Shoufa Chen, Chongjian Ge, Zhan Tong, Jiangliu Wang, Yibing Song, Jue Wang, and Ping Luo. Adaptformer: Adapting vision transformers for scalable visual recognition. *NeurIPS*, 2022.
- [4] Xinlei Chen, Saining Xie, and Kaiming He. An empirical study of training self-supervised vision transformers. In *ICCV*, 2021.
- [5] Matthias De Lange, Rahaf Aljundi, Marc Masana, Sarah Parisot, Xu Jia, Aleš Leonardis, Gregory Slabaugh, and Tinne Tuytelaars. A continual learning survey: Defying forgetting in classification tasks. *IEEE Transactions on Pattern Analysis and Machine Intelligence*, 44(7):3366–3385, 2022.
- [6] Jia Deng, Wei Dong, Richard Socher, Li-Jia Li, Kai Li, and Li Fei-Fei. Imagenet: A large-scale hierarchical image database. In *CVPR*, 2009.
- [7] Jacob Devlin, Ming-Wei Chang, Kenton Lee, and Kristina Toutanova. BERT: Pre-training of deep bidirectional transformers for language understanding. In *NAACL*, 2019.
- [8] Jiahua Dong, Lixu Wang, Zhen Fang, Gan Sun, Shichao Xu, Xiao Wang, and Qi Zhu. Federated class-incremental learning. In *CVPR*, 2022.
- [9] Alexey Dosovitskiy, Lucas Beyer, Alexander Kolesnikov, Dirk Weissenborn, Xiaohua Zhai, Thomas Unterthiner, Mostafa Dehghani, Matthias Minderer, Georg Heigold, Sylvain Gelly, Jakob Uszkoreit, and Neil Houlsby. An image is worth 16x16 words: Transformers for image recognition at scale. In *ICLR*, 2021.
- [10] Qiankun Gao, Chen Zhao, Yifan Sun, Teng Xi, Gang Zhang, Bernard Ghanem, and Jian Zhang. A unified continual learning framework with general parameter-efficient tuning. In *ICCV*, 2023.
- [11] Haiyang Guo, Fei Zhu, Wenzhuo Liu, Xu-Yao Zhang, and Cheng-Lin Liu. Pilora: Prototype guided incremental lora for federated class-incremental learning. *ECCV*, 2024.
- [12] Xu Han, Zhengyan Zhang, Ning Ding, Yuxian Gu, Xiao Liu, Yuqi Huo, Jiezhong Qiu, Liang Zhang, Wentao Han, Minlie Huang, et al. Pre-trained models: Past, present and future. *AI Open*, 2:225–250, 2021.
- [13] Kaiming He, Xinlei Chen, Saining Xie, Yanghao Li, Piotr Dollár, and Ross Girshick. Masked autoencoders are scalable vision learners. In *CVPR*, pages 16000–16009, 2022.
- [14] Dan Hendrycks, Steven Basart, Norman Mu, Saurav Kadavath, Frank Wang, Evan Dorundo, Rahul Desai, Tyler Zhu, Samyak Parajuli, Mike Guo, Dawn Song, Jacob Steinhardt, and Justin Gilmer. The many faces of robustness: A critical analysis of out-of-distribution generalization. *ICCV*, 2021.
- [15] Edward J Hu, Yelong Shen, Phillip Wallis, Zeyuan Allen-Zhu, Yuanzhi Li, Shean Wang, Lu Wang, and Weizhu Chen. LoRA: Low-rank adaptation of large language models. In *ICLR*, 2022.
- [16] Wenke Huang, Mang Ye, Zekun Shi, Guancheng Wan, He Li, Bo Du, and Qiang Yang. Federated learning for generalization, robustness, fairness: A survey and benchmark. *IEEE Transactions on Pattern Analysis and Machine Intelligence*, pages 1–20, 2024. doi: 10.1109/TPAMI.2024.3418862.
- [17] Menglin Jia, Luming Tang, Bor-Chun Chen, Claire Cardie, Serge Belongie, Bharath Hariharan, and Ser-Nam Lim. Visual prompt tuning. In *ECCV*, 2022.
- [18] Peter Kairouz, H Brendan McMahan, and etc. Advances and open problems in federated learning. *Foundations and Trends in Machine Learning*, 14(1–2):1–210, 2021.
- [19] Diederik P. Kingma and Jimmy Ba. Adam: A method for stochastic optimization. *CoRR*, abs/1412.6980, 2014.
- [20] James Kirkpatrick, Razvan Pascanu, Neil Rabinowitz, Joel Veness, Guillaume Desjardins, Andrei A Rusu, Kieran Milan, John Quan, Tiago Ramalho, Agnieszka Grabska-Barwinska, et al. Overcoming catastrophic forgetting in neural networks. *Proceedings of the National Academy of Sciences*, 114(13):3521–3526, 2017.
- [21] Brian Lester, Rami Al-Rfou, and Noah Constant. The power of scale for parameter-efficient prompt tuning. In *EMNLP*, 2021.
- [22] Qinbin Li, Yiqun Diao, Quan Chen, and Bingsheng He. Federated learning on non-iid data silos: An experimental study. In *IEEE International Conference on Data Engineering*, 2022.
- [23] Xiang Lisa Li and Percy Liang. Prefix-tuning: Optimizing continuous prompts for generation. In Chengqing Zong, Fei Xia, Wenjie Li, and Roberto Navigli, editors, *Proceedings of the 59th Annual Meeting of the Association for Computational Linguistics and the 11th International Joint Conference on Natural Language Processing (Volume 1: Long Papers)*, pages 4582–4597, Online, August 2021. Association for Computational Linguistics. doi: 10.18653/v1/2021.acl-long.353.
- [24] Zhizhong Li and Derek Hoiem. Learning without forgetting. *IEEE Transactions on Pattern Analysis and Machine Intelligence*, 40(12):2935–2947, 2018.
- [25] Zhuowei Li, Long Zhao, Zizhao Zhang, Han Zhang, Di Liu, Ting Liu, and Dimitris N. Metaxas. Steering prototypes with prompt-tuning for rehearsal-free continual learning. In *WACV*, 2024.
- [26] Marc Masana, Xialei Liu, Bartłomiej Twardowski, Mikel Menta, Andrew D. Bagdanov, and Joost van de Weijer. Class-incremental learning: Survey and performance

- evaluation on image classification. *IEEE Transactions on Pattern Analysis and Machine Intelligence*, 45(5):5513–5533, 2023. doi: 10.1109/TPAMI.2022.3213473.
- [27] Brendan McMahan, Eider Moore, Daniel Ramage, Seth Hampson, and Blaise Aguera y Arcas. Communication-efficient learning of deep networks from decentralized data. In *AISTATS*, 2017.
- [28] Hongming Piao, Yichen Wu, Dapeng Wu, and Ying Wei. Federated continual learning via prompt-based dual knowledge transfer. In *ICML*, 2024.
- [29] Daiqing Qi, Handong Zhao, and Sheng Li. Better generative replay for continual federated learning. In *ICLR*, 2023.
- [30] Sylvestre-Alvise Rebuffi, Alexander Kolesnikov, Georg Sperl, and Christoph H. Lampert. icarl: Incremental classifier and representation learning. In *CVPR*, 2017.
- [31] James Seale Smith, Leonid Karlinsky, Vyshnavi Gutta, Paola Cascante-Bonilla, Donghyun Kim, Assaf Arbelle, Rameswar Panda, Rogerio Feris, and Zsolt Kira. Codaprompt: Continual decomposed attention-based prompting for rehearsal-free continual learning. In *CVPR*, 2023.
- [32] James Seale Smith, Junjiao Tian, Shaunak Halbe, Yen-Chang Hsu, and Zsolt Kira. A closer look at rehearsal-free continual learning. In *CVPR*, 2023.
- [33] Jake Snell, Kevin Swersky, and Richard Zemel. Prototypical networks for few-shot learning. In *NeurIPS*, 2017.
- [34] Ashish Vaswani, Noam Shazeer, Niki Parmar, Jakob Uszkoreit, Llion Jones, Aidan N Gomez, Łukasz Kaiser, and Illia Polosukhin. Attention is all you need. In *NeurIPS*, 2017.
- [35] Catherine Wah, Steve Branson, Peter Welinder, Pietro Perona, and Serge Belongie. The caltech-ucsd birds-200-2011 dataset. 2011.
- [36] Liyuan Wang, Jingyi Xie, Xingxing Zhang, Mingyi Huang, Hang Su, and Jun Zhu. Hierarchical decomposition of prompt-based continual learning: Rethinking obscured sub-optimality. *NeurIPS*, 2023.
- [37] Liyuan Wang, Xingxing Zhang, Hang Su, and Jun Zhu. A comprehensive survey of continual learning: Theory, method and application. *IEEE Transactions on Pattern Analysis and Machine Intelligence*, pages 1–20, 2024. doi: 10.1109/TPAMI.2024.3367329.
- [38] Zifeng Wang, Zizhao Zhang, Sayna Ebrahimi, Ruoxi Sun, Han Zhang, Chen-Yu Lee, Xiaoqi Ren, Guolong Su, Vincent Perot, Jennifer Dy, and Tomas Pfister. Dualprompt: Complementary prompting for rehearsal-free continual learning. In *ECCV*, 2022.
- [39] Zifeng Wang, Zizhao Zhang, Chen-Yu Lee, Han Zhang, Ruoxi Sun, Xiaoqi Ren, Guolong Su, Vincent Perot, Jennifer Dy, and Tomas Pfister. Learning to prompt for continual learning. In *CVPR*, 2022.
- [40] Yue Wu, Yinpeng Chen, Lijuan Wang, Yuancheng Ye, Zicheng Liu, Yandong Guo, and Yun Fu. Large scale incremental learning. In *CVPR*, 2019.
- [41] Shipeng Yan, Jiangwei Xie, and Xuming He. Der: Dynamically expandable representation for class incremental learning. In *CVPR*, 2021.
- [42] Qiang Yang, Yang Liu, Tianjian Chen, and Yongxin Tong. Federated machine learning: Concept and applications. *ACM Trans. Intell. Syst. Technol.*, 10(2), jan 2019. ISSN 2157-6904. doi: 10.1145/3298981.
- [43] Jaehong Yoon, Eunho Yang, Jeongtae Lee, and Sung Ju Hwang. Lifelong learning with dynamically expandable networks. In *ICLR*, 2018.
- [44] Jaehong Yoon, Wonyong Jeong, Giwoong Lee, Eunho Yang, and Sung Ju Hwang. Federated continual learning with weighted inter-client transfer. In *ICML*, 2021.
- [45] Jiang-Tian Zhai, Xialei Liu, Andrew D Bagdanov, Ke Li, and Ming-Ming Cheng. Masked autoencoders are efficient class incremental learners. In *CVPR*, pages 19104–19113, 2023.
- [46] Jie Zhang, Zhiqi Li, Bo Li, Jianghe Xu, Shuang Wu, Shouhong Ding, and Chao Wu. Federated learning with label distribution skew via logits calibration. In *ICML*, 2022.
- [47] Jie Zhang, Chen Chen, Weiming Zhuang, and Lingjuan Lyu. Target: Federated class-continual learning via exemplar-free distillation. In *ICCV*, pages 4782–4793, 2023.
- [48] Yue Zhao, Meng Li, Liangzhen Lai, Naveen Suda, Damon Civin, and Vikas Chandra. Federated learning with non-iid data. *arXiv preprint arXiv:1806.00582*, 2018.
- [49] Da-Wei Zhou, Qi-Wei Wang, Han-Jia Ye, and De-Chuan Zhan. A model or 603 exemplars: Towards memory-efficient class-incremental learning. In *ICLR*, 2023.
- [50] Da-Wei Zhou, Zi-Wen Cai, Han-Jia Ye, De-Chuan Zhan, and Ziwei Liu. Revisiting class-incremental learning with pre-trained models: Generalizability and adaptivity are all you need. *IJCV*, 2024.
- [51] Da-Wei Zhou, Hai-Long Sun, Jingyi Ning, Han-Jia Ye, and De-Chuan Zhan. Continual learning with pre-trained models: A survey. In *IJCAI*, 2024. doi: 10.24963/ijcai.2024/924. Survey Track.
- [52] Da-Wei Zhou, Hai-Long Sun, Han-Jia Ye, and De-Chuan Zhan. Expandable subspace ensemble for pre-trained model-based class-incremental learning. In *CVPR*, 2024.
- [53] Jinghao Zhou, Chen Wei, Huiyu Wang, Wei Shen, Cihang Xie, Alan Yuille, and Tao Kong. ibot: Image bert pre-training with online tokenizer. *ICLR*, 2022.